CHIN. PHYS. LETT. Vol. 34, No. 7 (2017) 073201

# State Preparation in a Cold Atom Clock by Optical Pumping *

Yu-Xiong Duan(段玉雄)[1,2], Bin Wang(汪斌)[1**], Jing-Feng Xiang(项静峰)[1,2], Qian Liu(刘乾)[1,2], Qiu-Zhi Qu(屈求智)[1], De-Sheng Lü(吕德胜)[1], Liang Liu(刘亮)[1]

[1]*Key Laboratory of Quantum Optics, and Center for Cold Atom Physics, Shanghai Institute of Optics and Fine Mechanics, Chinese Academy of Sciences, Shanghai 201800*

[2]*University of Chinese Academy of Sciences, Beijing 100049*

(Received 20 April 2017)

*We implement optical pumping to prepare cold atoms in our prototype of the $^{87}$Rb space cold atom clock, which operates in the one-way mode. Several modifications are made on our previous physical and optical system. The effective atomic signal in the top detection zone is increased to 2.5 times with 87% pumping efficiency. The temperature of the cold atom cloud is increased by 1.4 $\mu$K. We study the dependences of the effective signal gain and pumping efficiency on the pumping laser intensity and detuning. The effects of $\sigma$ transition are discussed. This technique may be used in the future space cold atom clocks.*

*PACS:* 32.10.Fn, 32.80.Xx, 07.87.+v DOI: 10.1088/0256-307X/34/7/073201

Frequency instability is a key performance indicator of atomic clocks. In cold atom clocks, quantum projection noise and the Dick effect are the two main sources of frequency instability.[1] To reduce quantum projection noise, a larger number of effective cold atoms are desired in cold atom clocks. In the fountain clocks, only $m_{\rm F} = 0$ sublevel of the ground state is used as the clock state to avoid the Zeeman shift, while the launched cold atoms are evenly distributed in all the sublevels of one hyperfine ground state. In a conventional state selection regime, atoms in other sublevels ($m_{\rm F} \neq 0$) are removed to increase the signal-to-noise ratio of the clock.[2] The majority of the cold atoms are wasted in this stage. A similar issue exists in space cold atom clocks. Two-frequency optical pumping is a promising solution to this problem.[3,4]

This technique was primarily used in thermal beam clocks.[4,5] When the pumping laser is appropriately polarized, the target state will be a dark state, and population in other states will be transferred to the target state through spontaneous emissions. This pumping regime introduces an extra heating effect by randomly scattering photons. This heating effect increases the atom loss due to the atom cloud expansion and is not ignorable in the cold atom clock. Domenico *et al.* implemented the repumping laser in a 2D optical lattice geometry, in which Sisyphus cooling was introduced and the heat produced by optical pumping was removed.[6] Chalupczak *et al.* used the method of adiabatic transfer in the multilevel system to avoid the heating due to spontaneous emissions, which requires a Raman sideband cooling procedure in an optical lattice beforehand.[7] These methods are complicated to perform in a clock and limited in efficiency. A much simpler optical pumping stage was implemented in the $^{133}$Cs fountain frequency standard NPL-CsF2 without compensating for the heating effect, and a five-times effective cold atom signal was still achieved. The corresponding purity of the clock state was up to 97%.[8,9] The pumping stage was performed in the magneto-optical trap (MOT). This technique was adopted in NMIJ-F2 as well.[10] The design scheme of NIM6 also proposed a depumping–optical pumping procedure, allowing the state selection microwave cavity to be removed.[11] From another perspective, the time for loading cold atoms can be decreased to only a fraction of the original value with this method. The Dick effect will be reduced because of shorter dead time. As a result, this technique shows great flexibility in decreasing the quantum projection noise and the Dick effect. However, all of the above research is based on the Cs fountains. It is worth noting that the collision shift of Rb atoms is much smaller than that of Cs atoms, which makes Rb fountains very attractive. Our work complements the relevant research blank in the Rb system. Here we study the case in an $^{87}$Rb cold atom clock and introduce this technique to space applications.

In this Letter, we study the state preparation in an $^{87}$Rb cold atom clock by optical pumping. Firstly, our modified physical system and optical pumping scheme are introduced. Then the experimental results for various pumping laser parameters are presented and discussed. Further, the effects of $\sigma$ transition in our experiment are analyzed in detail. In the end, we predict the potential performance of this technique in the future cold atom clocks based on numerical estimation.

Our experiments are based on the principle prototype of the $^{87}$Rb space cold atom clock.[12–16] The transformed physical package is shown in Fig. 1. The device consists of an MOT chamber, a state selection microwave cavity, an optical pumping chamber, a ring microwave cavity[12] (Ramsey cavity), and a top detection chamber, from bottom to top. Since there is no suitable window for optical pumping at the MOT, our optical pumping chamber is constructed from the pre-

*Supported by the Fund from the Ministry of Science and Technology of China under Grant No 2013YQ09094304, and the Youth Innovation Promotion Association of Chinese Academy of Sciences.

**Corresponding author. Email: wangbin@mail.siom.ac.cn

© 2017 Chinese Physical Society and IOP Publishing Ltd

vious lower detection chamber and inherits its standing wave condition. Similar to the top detection chamber, the previous lower detection chamber consists of three standing wave fields and one travelling wave field for two-level detection. We replace the detection beams by the combination of pumping and repumping beams and add a half wave plate to let them pass through the PBS with final polarization parallel to the axial of the clock. The previous repumping channel is replaced by an extra detection beam for later temperature measurements. The pumping and repumping beams are easily derived from the original laser system through acousto–optic modulators and beam splitters. In our pumping experiments, the state selection microwave cavity remains inoperative and the detection beam in the lower detection zone is shut down. The pumping zone is screened from the Earth's magnetic field by two magnetic shields. The stray field is less than 0.4 μT. Extra coils are wound to provide a bias magnetic field of 20 μT in this region. With this bias field, the quantization axis during the optical pumping process remains consistent with the C-field in the Ramsey cavity.

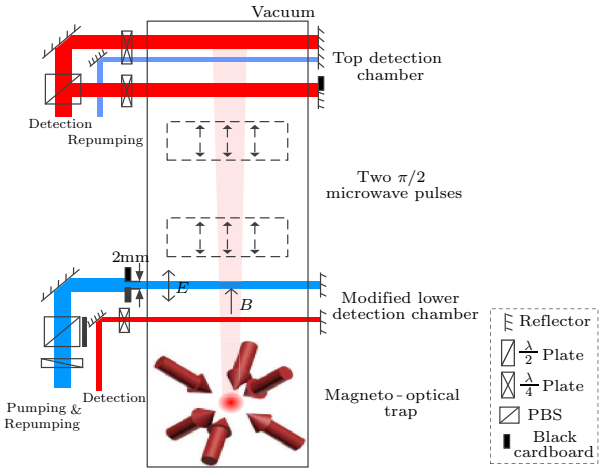


**Fig. 1.** Simplified schematic diagram of the transformed principle prototype clock. The state selection microwave cavity is hidden.

At the beginning of the clock operation period, the cold atoms are cooled and trapped in the bottom MOT. The three pairs of $\sigma^+ - \sigma^-$ cooling beams are arranged in the (1,1,1) configuration. After the loading phase, the MOT magnetic field is shut down, and then the atoms are launched by the moving molasses. Before leaving the MOT, the cold atoms are further cooled to a few μK by adiabatic cooling.[15] The atoms are equally populated in the five sublevels of $|F_g = 2\rangle$ after this stage. Then the atom cloud freely passes through the state selection cavity. Subsequently, most of the atoms are optically pumped to the clock state $|F_g = 2, m_f = 0\rangle$. The prepared atoms enter the following region of highly uniform C-field and experiences two coherent $\pi/2$ pulses in the ring microwave cavity, which is known as the separated oscillatory field (Ramsey) interrogation. In the end, the cold atoms arrive at the top detection chamber. The transition probability can be derived from the detected populations of the two clock states ($|F_g = 2, m_F = 0\rangle$ and $|F_g = 1, m_F = 0\rangle$). These populations are obtained from the two time-of-flight (TOF) fluorescence signals captured by two detectors, respectively. We can also obtain the temperature of the initial atomic cloud and that after optical pumping by Gaussian fitting of the TOF signals at the lower and top detection zone.[14] The previous device could also work in a fountain regime, but here we only study the one-way regime, which is the working mode in orbit.

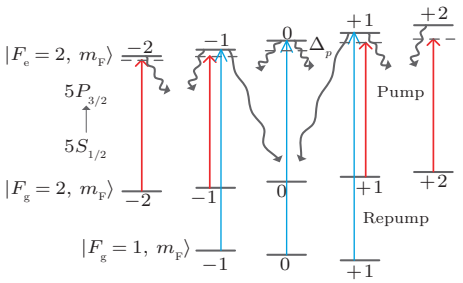


**Fig. 2.** Schematic diagram of optical pumping in our clock. The transition $|F_g = 2, m_F = 0\rangle \rightarrow |F_e = 2, m_F = 0\rangle$ is forbidden.

The schematic diagram of optical pumping is presented in Fig. 2. The $\pi$ polarized pumping laser is red-tuned from the $|F_g = 2\rangle \rightarrow |F_e = 2\rangle$ resonance on the D2 line of $^{87}$Rb by $\Delta_p$. The repumping laser is tuned to the $|F_g = 1\rangle \rightarrow |F_e = 2\rangle$ resonance and also $\pi$ polarized. The transition $|F_g = 2, m_F = 0\rangle \rightarrow |F_e = 2, m_F = 0\rangle$ is forbidden by the angular momentum selection rules. The atoms in other sublevels $|F_g = 2, m_F \neq 0\rangle$ are pumped to the excited states and spontaneously decay to the two ground states. A fraction of the atoms will decay to $|F_g = 2, m_F = 0\rangle$ and accumulate in this dark state. The resonant repumping laser is performed simultaneously to quickly excite the atoms in $|F_g = 1\rangle$, allowing the OP process to continue. After several loops of pumping and repumping, most of the atoms are prepared in the target clock state $|F_g = 2, m_F = 0\rangle$.[3,4] In the conventional $^{87}$Rb fountains, atoms in $|F_g = 2, m_F = 0\rangle$ are transferred to $|F_g = 1, m_F = 0\rangle$ by the microwave pulse, while atoms in other sublevels ($m_F \neq 0$) are finally removed by the state selection beam.[2] This means that less than 20% of the atoms are utilized. Optical pumping is able to transfer almost all the atoms from other sublevels to the clock state. Therefore, the number of effective atoms can be highly increased. In fact, the target clock state is not a perfect dark state because of the exciting neighboring transitions. Since the hyperfine energy splits between $|F_e = 2\rangle$ and $|F_e = 3, 1\rangle$ are limited (267 MHz and 157 MHz, respectively), the population leakage to these levels should be considered.[4,17–19] The method of using a narrow line width pumping beam tuned at the D1 line can reduce this effect (815 MHz between $|F_e = 2\rangle$ and $|F_e = 1\rangle$), but costs extra resources. Considering the Doppler effect, we here choose the negative pumping

detunings.

In our experiments, the atoms fly through the 2-mm-thick pumping beam at a velocity of 4 m/s. Thus the optical pumping duration is fixed at 0.5 ms. The repumping intensity $I_r$ is 3.27 mW/cm$^2$ and high enough to empty the population in $|F_g = 1\rangle$. After the optical pumping stage, the atoms are distributed in the hyperfine level $|F_g = 2\rangle$, and most of them are in sublevel $m_F = 0$. Using the Ramsey cavity, we separate the population of state $|F_g = 2, m_F = 0\rangle$ from the rest in the other sublevels ($m_F \neq 0$) of $|F_g = 2\rangle$. The frequency and power of the input microwave of the Ramsey cavity is set to make sure that the atoms in the state $|F_g = 2, m_F = 0\rangle$ are reversed to $|F_g = 1, m_F = 0\rangle$ after the Ramsey interrogation, based on the obtained Rabi oscillation pattern. At the upper detection zone, two TOF signals of the target sublevel and other sublevels are detected. We define the effective signal gain to be the ratio between the target sublevel populations obtained with and without optical pumping at the top detection chamber. The pumping efficiencies in this study refer to the ratio between the population in the sublevel $|F_g = 2, m_F = 0\rangle$ and the total population after the pumping procedure.

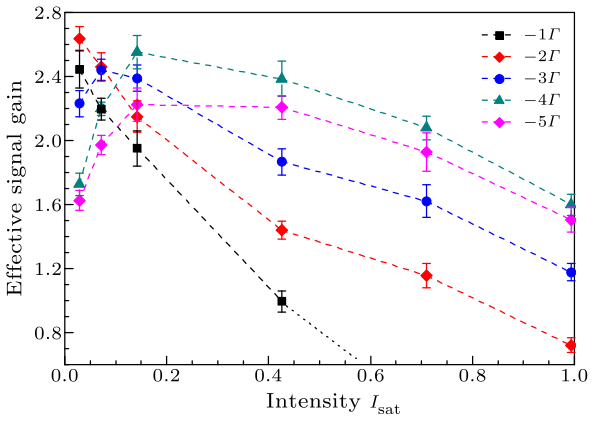


**Fig. 3.** Effective signal gains as a function of the pumping intensity for various pumping detunings. The natural line width $\Gamma$ is 6 MHz. The saturation intensity $I_{sat}$ is 3.27 mW/cm$^2$.

The results of effective signal gain for various pumping detunings and intensities are shown in Fig. 3. The signal gain for all pumping detunings tends to increase with the pumping intensity $I_p$ to a peak and then decrease. The reason is that sufficiently large intensity is required to fulfill pumping for each $\Delta_p$ in limited pumping duration. Therefore the peak appears at smaller $I_p$, when the pumping laser becomes closer to resonance. The peaks at detuning $-\Gamma$ and $-2\Gamma$ should also appear, if we extend our range to smaller intensity. The decrease of the gain at large $I_p$ is due to the heating effect. The heated atom cloud with a larger size decays more rapidly when travelling through the apertures of the vacuum system and microwave cavity. Further, the factor of $\sigma$ transition should be considered. A minor deviation of the pumping laser polarization or quantization axis can introduce $\sigma$ transitions to the pumping process. The $\sigma$ transition increases the target clock state leakage, causing extra heating.[8] As a result, the signal gain of near-resonance detuning $-\Gamma$ is smaller than that of $-2\Gamma$, and decreases more rapidly when $I_p$ increases. It is further supported by the results of pumping efficiency versus different pumping parameters given in Fig. 4(a). As $I_p$ increases, the pumping efficiency increases and finally reaches a steady level. When $I_p$ is large enough to reach maximum efficiency, further increasing $I_p$ will only increase the atom loss. As a result, the effective signal gain depends on the competition between efficiency and the heating effect.

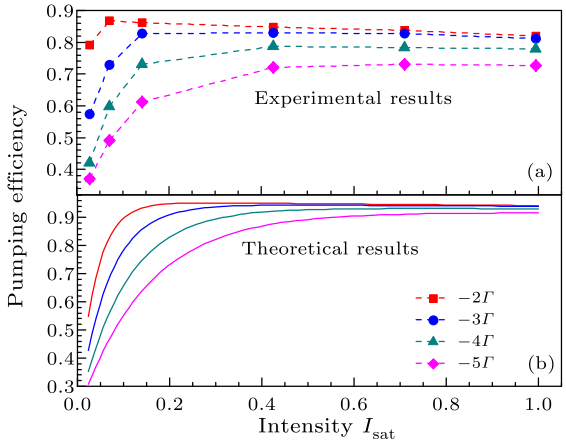


**Fig. 4.** Pumping efficiency as a function of pumping intensity at various pumping detunings.

In addition, the $\sigma$ transition builds coherence among ground state Zeeman sublevels.[20] The target dark state $|F_g = 2, m_F = 0\rangle$ is linked to all the other sublevels in $|F_g = 2\rangle$ by the $\sigma$ transitions. Several coherent $\Lambda$ configurations are formed with the $\sigma$ and $\pi$ transitions driven by the pumping laser. These coherences cause the coherent population trapping in other ground state sublevels ($m_F \neq 0$) in $|F_g = 2\rangle$. As shown in Fig. 4(a), the pumping efficiency is greatly reduced by the Zeeman coherence especially at large single photon detunings,[21] since the two-photon detuning of these coherences only depends on the Zeeman energy level split. In our experiment, the magnetic field is raised to 20 μT to lessen this effect. The theoretical efficiency without the $\sigma$ transition that can be achieved is over 98% by solving the density-matrix rate equations.[3,8]

Here we add $\sigma$ transition to our density-matrix rate equations as a perturbation term.[3] This method is applicable when the pumping frequency is neither too close nor too far from resonance. Initially, the atoms are equally distributed in the five sublevels of $|F_g = 2\rangle$, and the off-diagonal coherence terms are zero. By solving the density-matrix rate equations, we obtain the dynamics of the ground and excited state population during the pumping process. Considering the spontaneous emissions from the excited states, the temperature increase $\Delta T$ can be predicted through the average scattered photon number $n_{phot}$. Theoret-

ically, it is given by $\Delta T = T_{\rm recoil} n_{\rm phot}/3$, where $T_{\rm recoil}$ is the recoil temperature of $^{87}$Rb.[6–8] We choose two detunings of $-2\Gamma$ and $-3\Gamma$. The experimental and theoretical temperature increases of various pumping intensities are shown in Fig. 5. In comparison of the theoretical and experimental results, the $\sigma$ component is estimated to be 2%. We plug this 2% $\sigma$ transition back to our density-matrix rate equations, and obtain the predicted efficiency shown in Fig. 4(b). The experimental efficiencies agree well with those predicted by the rate equations in the low intensity range. The experimental steady efficiencies are lower than those predicted because the Zeeman coherence is not included in the theoretical model. A precise model considering two-frequency pumping combined with the Zeeman coherence introduced by additional $\sigma$ transitions is complicated and beyond the scope of this work. It is worth noting that the theoretical pumping efficiency slightly decreases in the large pumping intensity range. The reason is that the pumping and repumping lasers also form $\Lambda$ configurations.[8] However, they are independent lasers with estimated line width of 500 kHz, and the two-photon detuning depends on pumping detuning $\Delta_{\rm p}$. Here $\Delta_{\rm p}$ is below $-\Gamma$. Thus this factor has less influence on efficiency compared with the Zeeman coherence. The above results and discussions are also suitable to the fountain regime.

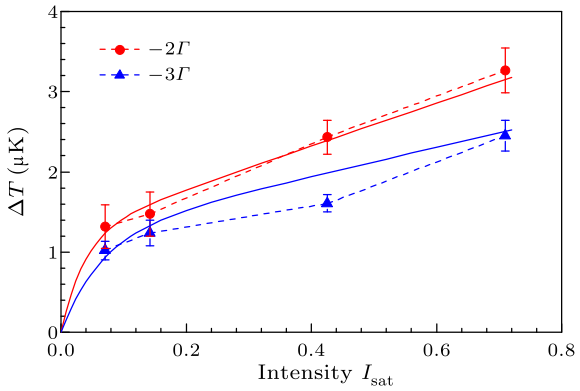


**Fig. 5.** Temperature increase as the function of pumping intensity for detuning $-2\Gamma$ and $-3\Gamma$. The solid lines represent the theoretical predictions with 2% $\sigma$ transition. The dashed lines and symbols represent the experimental results.

Considering both the signal gain and efficiency, the optimal result achieved is an effective gain of 2.5 with 87% efficiency when $I_{\rm p}$ is $0.07 I_{\rm sat}$ and $\Delta_{\rm p}$ is $-2\Gamma$. It means that the effective cold atoms are increased to 4.35 times at the pumping zone but this ratio decreases to 2.5 at the top detection zone due to the heating effect. Here the effective gain is smaller than that achieved in the Cs fountain mainly due to fewer magnetic sublevels.[8] In the systems mainly limited by the quantum projection noise, such as an Rb fountain in which atoms are cooled and captured directly by molasses, the clock stability can be approximately improved by a factor of $\sqrt{2.5}$, which is 1.6. In other cases, the contributions of other noises should also be considered. Figure 6 shows a comparison between the TOF signals with and without optical pumping. Higher effective signal gain is achieved at smaller $I_{\rm p}$, but the corresponding efficiency is below 80%. We hope to increase the pumping efficiency towards the theoretical limit of 98% by eliminating the $\sigma$ component. Our present improvements are limited by the previous compact structure. In practical applications, this optical pumping stage can be realized in the MOT under sequential control and the state selection cavity is not needed any more.

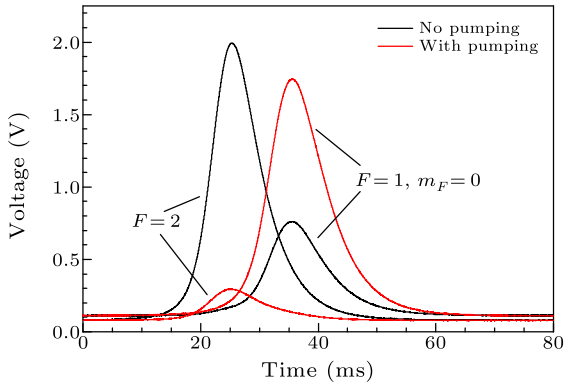


**Fig. 6.** TOF signals obtained with and without optical pumping. The corresponding pumping parameters $I_{\rm p}$ and $\Delta_{\rm p}$ are $0.07 I_{\rm sat}$ and $-2\Gamma$.

Here we extend this technique to the $^{87}$Rb space cold atom clock in space.[16] Since the atom cloud flies at a constant slow speed in microgravity, the removal of state selection cavity in the new configuration can reduce the dead time of the clock and directly improve the clock stability. Moreover, the relationship between the atom cloud size and temperature $T$ is given by

$$T = \frac{M}{\kappa_{\rm B}} \sigma_{\rm v}^2, \tag{1}$$

$$\sigma_L^2 = \sigma_0^2 + \sigma_{\rm v}^2 \left(\frac{L}{v}\right)^2, \tag{2}$$

where $M$ is the atomic mass, $\kappa_{\rm B}$ is the Boltzmann constant, $v$ is the launching velocity, $L$ is the distance from the launch site to the detection zone, $\sigma_0$ and $\sigma_L$ are the cloud Gaussian radiuses at the launch site and the top detection chamber, and $\sigma_{\rm v}$ is the expansion velocity of the cloud. As shown in Fig. 7, in the new configuration, the flying distance $L$ will be decreased to $L'$. From Eqs. (1) and (2) we can derive the equation

$$\frac{\sigma_{L'}^2 - \sigma_0^2}{\sigma_L^2 - \sigma_0^2} = \left(\frac{L'}{L}\right)^2 \frac{T_0 + \Delta T}{T_0}, \tag{3}$$

where $T_0$ is the initial atom temperature. In a typical case in space, $T_0 = 2.5\,\mu$K, $\frac{L'}{L} = 0.8$, and $\Delta T = 1.4\,\mu$K. The corresponding value of $\frac{\sigma_{L'}^2 - \sigma_0^2}{\sigma_L^2 - \sigma_0^2}$ will be 0.9984. Hence in microgravity, the optically pumped atomic cloud can reach the detection zone even without increasing its cloud size compared with

the size in the conventional configuration regardless of the launching velocity. A nearly five-fold effective signal gain is expected in the $^{87}$Rb space cold atom clock in orbit, which is comparable with the gain achieved in the Cs fountain on the ground.[8] Furthermore, the size and weight of the system will be decreased, which is an important aspect in space applications.

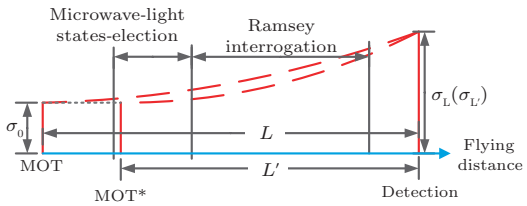


**Fig. 7.** Schematic diagram of cloud expansion along the flying path. The MOT in the new configuration is marked with the asterisk.

In conclusion, we have experimentally and theoretically studied the dependence of signal gain and pumping efficiency on the pumping intensity and detuning. We achieve a 2.5 times effective signal gain with pumping efficiency of 87% at the optimal pumping laser intensity and detuning. The cold atoms are heated by 1.4 μK. The existing $\sigma$ transitions increase the target clock state leakage, introduce extra heat and lead to the Zeeman coherence. Our effective signal gain and pumping efficiency will be further improved by reducing the $\sigma$ transition component. Similar results can be expected in the $^{87}$Rb fountain clock. Our numerical estimation predicts a nearly five-fold atomic signal gain in the new configuration of $^{87}$Rb space cold atom clock in orbit. The above results and discussions based on the $^{87}$Rb systems are also instructive for the systems of other alkali species.

The authors would like to thank Professor Jun Qian and Professor Shuyu Zhou for their valuable discussions and Yuanyuan Yao for her strong support in electronics.

## References

[1] Riehle F 2006 *Frequency Standards: Basics and Applications* (John Wiley & Sons) chap 7 p 223
[2] Wynands R and Weyers S 2005 *Metrologia* **42** S64
[3] Tremblay P and Jacques C 1990 *Phys. Rev.* A **41** 4989
[4] Avila G et al 1987 *Phys. Rev.* A **36** 3719
[5] Ohshima S, Nakadan Y S and Koga Y 1988 *IEEE Trans. Instrum. Meas.* **37** 409
[6] Di Domenico G et al 2010 *Phys. Rev.* A **82** 053417
[7] Chalupczak W and Szymaniec K 2005 *Phys. Rev.* A **71** 053410
[8] Szymaniec K et al 2013 *Appl. Phys.* B **111** 527
[9] Szymaniec K and Park S E 2011 *IEEE Trans. Instrum. Meas.* **60** 2475
[10] Takamizawa A et al 2015 *IEEE Trans. Instrum. Meas.* **64** 2504
[11] Fang F et al 2015 *Frequency Control Symposium & the European Frequency and Time Forum (FCS), 2015 Joint Conference of the IEEE International* (Denver, USA 12–16 April 2015) p 492
[12] Ren W et al 2016 *Chin. Phys.* B **25** 060601
[13] Qu Q Z et al 2015 *Chin. J. Laser* B **42** 0902006 (in Chinese)
[14] Lü D S et al 2011 *Chin. Phys. Lett.* **28** 063201
[15] Wang B et al 2011 *Chin. Phys. Lett.* **28** 063701
[16] Qu Q Z et al 2015 *Chin. Opt. Lett.* **13** 061405
[17] Zhang S S et al 2016 *Chin. Phys.* B **25** 114203
[18] Wang L R et al 2015 *Chin. Phys.* B **24** 063201
[19] Wang P J et al 2011 *Chin. Phys.* B **20** 016701
[20] Théobald G et al 1989 *Opt. Commun.* **71** 256
[21] Dalton B J, McDuff R and Knight P L 1985 *Opt. Acta* **32** 61